An Infrared Search for Dust-Extinguished SNe in ULIRG Galaxies

Ori D. Fox (STScI) & Harish Khandrika (STScI)

Supernova (SN) rates serve as an important probe of star formation models and initial mass functions, particularly at high redshifts due to the SN intrinsic luminosity. Ground-based optical surveys, however, typically discover nearly ten times fewer SNe than predicted, challenging our understanding of massive star formation and evolution. These results are generally attributed to the high dust extinction associated with the nuclei of star forming galaxies, such as Ultra Luminous InfraRed Galaxies (ULIRGs). A successful survey must be conducted at longer wavelengths and with a space-based telescope, which has stable seeing that reduces the necessity for any subtraction algorithms and, therefore, residuals. WFIRST offers an ideal instrument to conduct this experiment. Here we present ongoing work from our 300 hour Spitzer 3.6 micron survey for dust-extinguished SNe in the nuclear regions of ULIRGs within 200 Mpc. The direct product of this study will lay the groundwork for a future survey with WFIRST.

Missing SNe

The observed rate at which stars more massive than 8 $M_\odot$ explode as core-collapse supernovae (CCSNe) can be used to determine chemical evolution and feedback processes, progenitor mass distributions, star-formation rates, and dust yields.

The ability to detect all SNe in a survey limits the completeness of any rate study. This is particularly true in galaxies with high star-formation rates, where gas and dust obscure most of the SNe. In fact, visible-wavelength surveys for SNe in dusty starburst galaxies have established SN rates that are unexpectedly similar to rates observed in more normal galaxies.

The IR, which is about 10 times less affected by extinction than visible light, offers an optimized window for SN searches in these starburst galaxies. In general, the results highlight that $\sim$80\% of nearby SNe remain hidden within the innermost nuclear regions of galaxies, with dust extinction A_V > 25 mag.

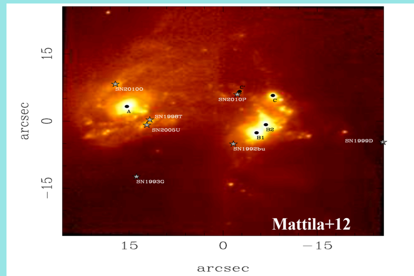

Figure 1: HST/NICMOS F164N image (from Alonso-Herrero et al. 2000) of Arp 299 shown with a square-root scaling to emphasize the extent of the diffuse emission in the circumnuclear regions. This image traces the CCSN activity via the [Fe II] 1.644 μm line. The positions of the main nuclei A, B1 and B2, sources C and C', and the SNe discovered at optical or IR wavelengths are indicated.

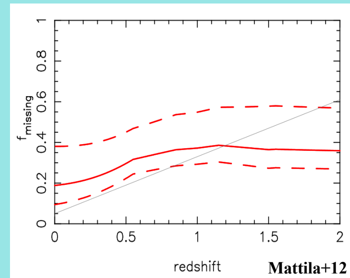

Figure 2: Fraction of SNe missed by rest-frame optical searches as a function of redshift. Red lines show our best (Nominal) estimate together with Low and High missing fraction models as dashed lines. Solid black line is the missing fraction from Mannucci et al. (2007).

The advantage of the Infrared (even WFIRST!)

IRAC Channel 1 (3.6 μm) provides an optimal window for detecting SNe embedded in the nuclei of ULIRGs. Increasing extinction (A > 25 mag) shifts the peak of the observed spectrum out beyond the K-band (2.1 μm). Due to the rising thermal background past 2 μm, it is difficult to achieve the same sensitivity with ground-based observations.

A space-based survey offers stable seeing, which reduces the necessity for template subtractions to detect SNe in the galactic nuclei.

We have compiled a list of 41 ULIRGs to be monitored for SNe and other transients over two years. To achieve the desired statistics, we request each galaxy be observed 8 times at t_{int} = 3200 s.

Table 1: Results With 16 Expected SNe

Number of SNe Detected	Statistics	Lessons
<4	$> 3\sigma$	*proof* that SNe are still hidden and/or rates miscalculated
4-8	$2-3\sigma$	*likely* that some SNe are still hidden and/or rates miscalculated
8-12	$1-2\sigma$	*possibility* that some SNe are still hidden and/or rates miscalculated
12-20	$\pm1\sigma$	observations consistent with expectations
20-24	$1-2\sigma$	*possible* underestimate of SN rate
24-28	$2-3\sigma$	*likely* underestimate of SN rate
>28	$> 3\sigma$	*proof* of error in SN rate

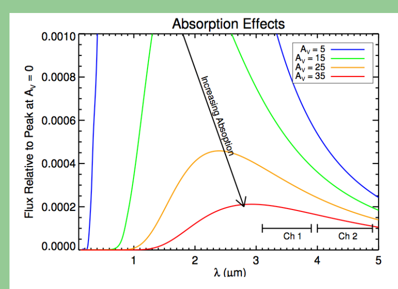

Figure 3: The effects of dust on the intensity and shape of a blackbody spectrum. The plotted flux is scaled relative to the peak flux at A_V = 0 mag. Since more absorption occurs at shorter wavelengths, the peak of the blackbody spectrum shifts beyond the near-infrared (i.e., 2.1 um) as A_V increases > 25. For these extinction levels, Spitzer/IRAC Channel 1 (3.6 um) provides an optimal window for detecting SNe.

Figure 4: The expected signal-to-noise ratio for the limiting scenario: a 5400 K blackbody at 200 Mpc with an A_V = 35. The noise corresponds to Poisson noise from the underlying ULIRG, which we model after measurements of Arp 220 (Scoville et al., 1998). The plot shows that we can maintain a SNR > 5 out to 200 Mpc with a 3240s integration.

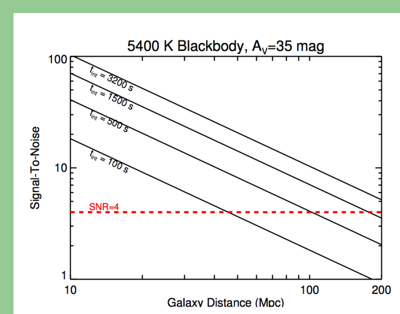

Preliminary Results

Despite the stable seeing from space, the *Spitzer* PSF itself is not (even close to) symmetric. The telescope rotation throughout the year therefore makes it difficult to search for SNe using standard template subtraction techniques, especially towards the galactic nuclei where most obscured SNe tend to exist.

Instead, we developed a SN detection algorithm using aperture photometry techniques. The noise, however, was dominated by systematics in the data that took significant time to remove and, ultimately, to reduce to the original statistical noise predicted in the proposal.

We present here some preliminary results of the algorithm that will be applied to all the data in the near future. While *WFIRST* does not extend to the mid-IR, it does offer a much more symmetric and higher-resolution PSF with which to do this project with almost no additional cost.

Figure 5: The asymmetric Spitzer PSF complicates the search for SNe using template subtraction techniques. Instead, we develop an aperture photometry detection algorithm.

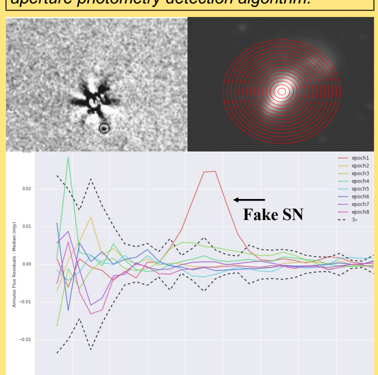

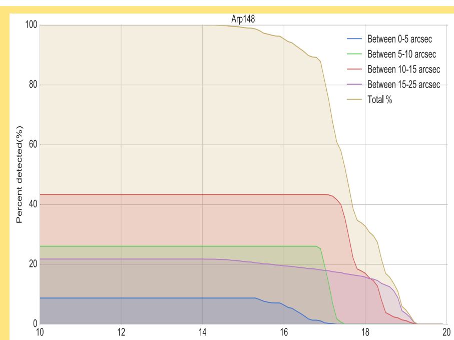

Figure 6: Preliminary results showing the completeness of our aperture detection algorithm. Fake SNe are planted in a grid across the galaxy and recovered using the algorithm. This plot shows the percentage of SNe detected as a function of magnitude for various radius bins.